International Journal of Pharmaceutics 477 (2014) 236–243

Contents lists available at ScienceDirect

International Journal of Pharmaceutics

journal homepage: www.elsevier.com/locate/ijpharm

Pharmaceutical nanotechnology

A novel ibuprofen derivative with anti-lung cancer properties: Synthesis, formulation, pharmacokinetic and efficacy studies

Ka-Wing Cheng [a,1], Ting Nie [a,1], Nengtai Ouyang [a,b], Ninche Alston [a], Chi C. Wong [a,c], George Mattheolabakis [a], Ioannis Papayannis [a], Liqun Huang [a], Basil Rigas [a,*]

[a] Division of Cancer Prevention, Department of Medicine, Stony Brook University, Stony Brook, NY, USA
[b] Medicon Pharmaceuticals, Inc., Stony Brook, NY, USA
[c] Department of Medicine and Therapeutics, Chinese University of Hong Kong, Hong Kong

ARTICLE INFO

Article history:
Received 9 May 2014
Received in revised form 22 July 2014
Accepted 7 October 2014
Available online 11 October 2014

Keywords:
Lung cancer
Liposome
Phospho-ibuprofen amide
Ibuprofen
Xenografts

ABSTRACT

Phospho-non-steroidal anti-inflammatory drugs (phospho-NSAIDs) are a novel class of NSAID derivatives with potent antitumor activity. However, phospho-NSAIDs have limited stability *in vivo* due to their rapid hydrolysis by carboxylesterases at their carboxylic ester link. Here, we synthesized phospho-ibuprofen amide (PIA), a metabolically stable analog of phospho-ibuprofen, formulated it in nanocarriers, and evaluated its pharmacokinetics and anticancer efficacy in pre-clinical models of human lung cancer. PIA was 10-fold more potent than ibuprofen in suppressing the growth of human non-small-cell lung cancer (NSCLC) cell lines, an effect mediated by favorably altering cytokinetics and inducing oxidative stress. Pharmacokinetic studies in rats revealed that liposome-encapsulated PIA exhibited remarkable resistance to hydrolysis by carboxylesterases, remaining largely intact in the systemic circulation, and demonstrated selective distribution to the lungs. The antitumor activity of liposomal PIA was evaluated in a metastatic model of human NSCLC in mice. Liposomal PIA strongly inhibited lung tumorigenesis (>95%) and was significantly ($p < 0.05$) more efficacious than ibuprofen. We observed a significant induction of urinary 8-iso-prostaglandin $F_{2\alpha}$ *in vivo*, which indicates that ROS stress probably plays an important role in mediating the antitumor efficacy of PIA. Our findings suggest that liposomal PIA is a potent agent in the treatment of lung cancer and merits further evaluation.

1. Introduction

Lung cancer is the leading cause of cancer related deaths in both males and females in the United States of America, accounting for approximately 30% of all deaths due to cancer (Jemal et al., 2010). Epidemiological studies have shown that daily administration of ibuprofen, a non-steroidal anti-inflammatory drug (NSAID) reduces the risk of lung cancer (Harris et al., 2007). As with most NSAIDs, however, long term use of ibuprofen is associated with significant side effects, most prominently gastrointestinal and renal toxicity (Henry and McGettigan, 2003; Wolfe et al., 1999; Yoshikawa and Naito, 2011). Our group has developed novel derivatives of NSAIDs, such as phospho-ibuprofen (PI), by covalently attaching to NSAIDs a diethyl-phosphate moiety via a spacer molecule.

PI has demonstrated enhanced anticancer efficacy over ibuprofen in inhibiting the growth of human colon cancer cell lines *in vitro* and in human colon cancer xenografts in mice, without any significant gastrointestinal toxicity (Xie et al., 2011). However, its efficacy *in vivo* is suboptimal due to its poor pharmacokinetic properties. Specifically, rapid hydrolysis by blood esterases and its poor solubility render the bioavailability of intact PI below 5% (Wong et al., 2012). Herein, we have synthesized phospho-ibuprofen-amide (PIA), a metabolically stable amide analog of PI, formulated it in liposomes, and evaluated the pharmacokinetics and anticancer efficacy of liposome-encapsulated PIA.

Incorporation of drugs in nanocarriers, such as liposomes (Flenniken et al., 2006; Gabizon, 2001), dendrimers (Lee et al., 2005) and polymeric micelles (Blanco et al., 2009; Sutton et al., 2007), is a promising approach to overcome the limitations of

Abbreviations: DCF-DA, 2,7-dichlorofluorescein diacetate; 8-iso-$PGF_{2\alpha}$, 8-iso-prostaglandin $F_{2\alpha}$; NSAIDs, Non-steroidal anti-inflammatory drugs; NSCLC, Non-small-cell lung cancer; PIA, Phospho-ibuprofen amide; ROS, Reactive oxygen species.

* Corresponding author at: Division of Cancer Prevention, HSC, T-17 Room 080, Stony Brook, New York, USA. 11794-8173. Tel.: +1 631 444 9538; fax: +1 631 444 9553.
E-mail address: basil.rigas@stonybrook.edu (B. Rigas).

[1] These authors contributed equally to this work.

http://dx.doi.org/10.1016/j.ijpharm.2014.10.019
0378-5173/

many anticancer drugs related to poor water solubility and metabolic instability (Alexis et al., 2010; Peer et al., 2007). Recent studies have shown that bioavailability and efficacy of poorly soluble lipophilic anticancer agents can be improved by incorporation in β-lapachone micelles (Blanco et al., 2010) and liposomes (Mattheolabakis et al., 2012). The increased blood solubility of these modified nanoparticles and the subsequent prolonged circulation time decrease the dose needed to achieve the equivalent pharmacological effect of the free compound. Our group has demonstrated the successful use of liposomes to improve the bioavailability and efficacy of PI (Nie et al., 2012). Given the structural similarity between PI and PIA, we hypothesized that the efficacy of PIA could be significantly improved using liposome as a delivery vehicle.

Herein, we describe the synthesis and liposomal formulation of PIA, a novel derivative of ibuprofen and report on its pharmacokinetic properties and efficacy in suppressing lung cancer in preclinical models.

2. Material and methods

2.1. Reagents

All reagents and solvents were of ACS grade. ^{1}H NMR spectra were recorded on a Varian 400 spectrometer. Samples prepared for NMR analysis were dissolved in $CDCl_3$. Chemical shifts are reported in ppm relative to TMS. Electron ionization mass spectra were recorded on a Thermo Scientific DSQ (II) mass spectrometer. Thin-layer chromatography (TLC) was performed on silica gel sheets (Tiedel-deHaën, Sleeze, Germany) containing a fluorescent indicator. Flash column chromatographic separations were carried out using 60 Å silica gel (TSI Chemical Company, Cambridge, MA). All experiments dealing with moisture- or air-sensitive compounds were conducted under dry nitrogen. Proliferating cell nuclear antigen (PCNA) antibody was from Cell Signaling (Danvers, MA). Trx-1 and Trx-R antibodies were from Abcam (Cambridge, MA).

2.2. Synthesis of PIA

2.2.1. Synthesis of N-(4-hydroxy-butyl)-2-(4-isobutyl-phenyl)-propionamide

Ibuprofen (0.228 g, 1 mmol), 3-amino propanol (0.138 mL, 1.5 mmol) and enzotriazole-*N*,*N*,*N*′,*N*′-tetramethyl-uronium-hexafluoro-phosphate (HBTU, 0.57 g, 1.5 mmol) were dissolved in 5 mL of DMF containing diisopropylethylamine (DIPEA, 0.17 mL, 1 mmol). The reaction mixture was stirred at room temperature for 4 h. The reaction was monitored by TLC. The remnant was dissolved in ethyl acetate, and then washed sequentially with 1 M HCl, saturated $NaHCO_3$, distilled water, and brine, and dried over anhydrous sodium sulfate (Na_2SO_4). After the solvent was removed, the crude product was purified by flash column chromatography to give *N*-(4-hydroxy-butyl)-2-(4-isobutyl-phenyl)-propionamide as a white solid with a 95% yield. ^{1}H NMR ($CDCl_3$): δ 0.9 (s, 6H), 1.3 (d, 3H), 1.6 (m, 4H), 1.8 (m, 5H), 2.5 (d, 2H), 3.6 (m, 1H), 4.05 (m, 4H), 5.5 (s, 1H), 7.1 (d, 2H), and 7.2 (d, 2H).

2.2.2. Synthesis of phosphoric acid diethyl ester 4-[2-(4-isobutyl-phenyl)-propionylamino]-butyl ester

Under nitrogen, diethylchlorophosphate (0.43 g, 1.25 mmol) was added drop-wise to a solution of alcohol (**1e**, 0.299 g, 1 mmol) in dichloromethane (10 mL) containing diisopropylethylamine (0.17 mL, 1 mmol) and 4-(dimethylamino) pyridine (6 mg, 0.05 mmol). The reaction mixture was stirred overnight. The reaction solution was washed with water (2 × 25 mL), dried over anhydrous Na_2SO_4, filtered and concentrated. The crude residue was purified by silica gel open column chromatography using hexane:ethyl acetate (60:40, v/v) as the eluant. Fractions were collected and their profiles were checked by high-performance liquid chromatography (HPLC). The pure fractions were combined and evaporated to give a slightly yellow liquid with a percent yield of 85%. ^{1}H NMR ($CDCl_3$): δ 0.9 (s, 6H), 1.2 (m, 6H), 1.3 (d, 3H), 1.6 (m, 4H), 1.8 (m, 5H), 2.5 (d, 2H), 3.6 (m, 1H), 4.05 (m, 8H), 5.5 (s, 1H), 7.1 (d, 2H), and 7.2 (d, 2H).

2.3. Preparation of liposome-encapsulated PIA

Liposomes were prepared as previously described (Nie et al., 2012). Briefly, Soy-PC, DSPE–PEG (1,2-distearoyl-sn-glycero-3-phosphoethanolamine-*N*-[amino(polyethylene glycol)-2000]; ammonium salt) and PIA were dissolved in chloroform. The solution was evaporated to a thin film, rehydrated with phosphate buffered saline (PBS) and gradually extruded through double polycarbonate membranes of 0.08- or 0.02-μm pore size (Waters, Milford, MA) using an extruder device (Lipex Biomembranes, Vancouver, BC, Canada). The final concentration of each component was 37 mg/mL Soy-PC, 7.4 mg/mL DSPE–PEG and 20 mg/mL PIA. The non-encapsulated PIA was separated from liposomes by extensive dialysis against saline. The liposomes were freeze-dried in a LABCONCO freeze drier (LABCONCO Co., Kansas, Missouri) under the following conditions: −40 °C, 50 mTorr. The amounts of PIA incorporated into liposomes were determined by HPLC. The molar ratios between soy PC, DSPE–PEG and PIA were determined by ^{1}H NMR spectroscopic analysis of freeze-dried liposomal PIA.

2.4. Characterization of liposomal PIA

Size distribution of PIA-encapsulated liposomes was measured by dynamic light scattering, using Zeta Plus with the BI-MAS option (Brookhaven Instruments Co., Holtsville, NY). All measurements were performed in triplicate at 25 °C at a measurement angle of 90°. The morphology of liposomes was examined by transmission electron microscopy (TEM) with negative staining. Briefly, the samples were prepared by wetting a carbon-coated grid with a small drop of a diluted liposome or micelle solution. Upon drying, they were stained with 1% uranyl acetate and 2% phosphotungstic acid, air-dried at room temperature and viewed under a FEI BioTwinG2 electron microscope (FEI, Hillsboro, OR).

2.5. Cell culture

A549, H23 and H358 human non-small-cell lung cancer (NSCLC) cell lines were purchased from American Type Culture Collection (ATCC, Manassas, VA). A549 was cultured in F12K medium and H23 and H358 in RPMI medium, as recommended by ATCC.

2.6. Cytokinetic analyses

Cell viability was measured with the MTT assay (Roche Diagnostics, Indianapolis, IN). For cell cycle analysis, cells were fixed using cold 70% ethanol and stained with PI following standard protocols prior to flow cytometric analysis. Apoptosis and necrosis were assessed by staining cells with Annexin V-FITC and propidium iodide (PI) and analyzing them by flow cytometry following standard protocols (Kozoni et al., 2000).

2.7. Oxidative stress assay

Reactive oxygen and nitrogen species (RONS) levels in cultured cells were determined using the general RONS probe dichlorodihydrofluorescein diacetate (DCF-DA). A549, H23 or H358 cells treated with PIA for 1.5 h were loaded with DCF-DA, and

fluorescence intensity was analyzed on a FACScaliber following standard protocols (BD Bioscience).

The effect of PIA or liposomal PIA on the redox state of the mice bearing orthotopic lung tumors was assessed by measuring the levels of urinary 8-iso-prostaglandin $F_{2\alpha}$ (8-iso-$PGF_{2\alpha}$) using an ELISA kit (Oxford Biomedical Research, MI, USA).

2.8. Pharmacokinetic and tissue distribution studies

A single dose of PIA 200 mg/kg suspended in corn oil was given to mice by i.p. injection. Liposomal PIA was administered to rats with a single i.v. dose of 200 mg/kg. After treatment, the animals were sacrificed at designated time points, and blood was collected and immediately centrifuged to obtain the plasma. Acetonitrile (2× the volume of plasma) was added to the plasma samples, mixed and centrifuged at 13,000 × *g* for 15 min. The supernatants were analyzed by HPLC.

For analysis of tissue distribution, PIA was administered to mice by i.p. injection and liposomal PIA by i.v. injection, and the animals were euthanized 1 h post treatment. Organs were excised and snap-frozen in liquid nitrogen and stored at −80 °C until analysis. Accurately weighed amounts of the organs were homogenized individually in PBS (pH 7.4), sonicated, and extracted with acetonitrile. Subsequent steps for drug level determination were the same as those applied to the plasma samples.

2.9. In vivo *efficacy in lung cancer xenografts*

All animal experiments were performed with the approval of the Institutional Animal Care and Use Committee, State University of New York at Stony Brook. Female athymic nude mice (6–7 weeks old) were purchased from Harlan (Harlan Industries, Indianapolis, IN). After acclimation for 1 week, 6×10^6 A549 cells were injected i.v. into the tail vein of the animals. Two weeks post implantation when the tumors were established in the lungs (monitored by fluorescence imaging; Maestro, Wobum, MA), the mice were randomized into the vehicle and PIA treatment groups ($n = 6$). PIA was suspended in corn oil and given to the animals by i.p. injection at a dose of 200 mg/kg, once per day, five days per week for 6 weeks.

To evaluate whether liposomal incorporation of PIA could improve its anticancer efficacy and whether PIA is significantly better than its parent NSAID ibuprofen, we performed another study using the following treatment groups: vehicle, ibuprofen and liposomal PIA, which were administered to the animals by tail vein injection once a week at 200 mg/kg.

At sacrifice, lungs and tumors were excised from the animals and their images were taken on the Maestro imaging machine. Immediately following this step, the lungs (including the orthotopic xenografts) and other organs/tissues were snap-frozen in liquid nitrogen or preserved in formalin for subsequent analysis.

2.10. Immunohistochemistry

Tissue samples were fixed in 10% buffered formalin and embedded in paraffin, and 4 μm-thick sections were placed on slides. The tissue sections were dewaxed and rehydrated according to standard protocols. The expression of PCNA, Trx-1 and Trx-R was determined by immunohistochemistry (IHC) staining following standard protocols. Scoring was performed according to the method reported in our previous study (Huang et al., 2011).

2.11. Statistical analyses

Data are expressed as mean ± SEM. Results were analyzed using the Student's t-test. P values <0.05 were considered statistically significant.

3. Results

3.1. Preparation and characterization of liposomal PIA

Liposomal PIA was prepared as described in Section 2. PIA is more hydrophobic compared to ibuprofen (octanol–water partition coefficient, Log $P = 4.78$ vs. 3.75), and thus could be more efficiently incorporated in liposomes. The average hydrodynamic radius of PIA-encapsulated liposomes was 220 nm. Negative-staining TEM (Fig. 1A) shows that the liposomes were homogenous, unilamellar and round vesicles with average diameter in accordance with the hydrodynamic diameter. The lipid to drug loading ratio of liposomal PIA was determined by ^{1}H NMR spectroscopy to be 1:1. In contrast, ibuprofen was virtually incompatible with the liposome carrier as evidenced by a 1:0 lipid to drug ratio. As shown in Fig. 1B, cellular uptake of PIA was much higher than that of ibuprofen (18 ± 1.2 vs. 0.1 ± 0.05 nmol/mg protein, mean ± SEM for this and all subsequent values), and liposomal formulation of PIA further enhanced its already superior uptake by over 4-fold.

3.2. PIA inhibits the growth of NSCLC human lung cancer cells

To evaluate the effect of the chemical modification of ibuprofen on its anticancer activity, we determined the 24-h IC_{50} values of PIA and ibuprofen in A549, H23 and H358 NSCLC cell lines (Fig. 1C). PIA demonstrated a substantially enhanced cytotoxicity (7- to >14-fold) compared to ibuprofen in the three cell lines. The potent growth inhibitory effect of PIA results from its cytokinetic effect. At 1.5 × IC_{50}, PIA significantly induced apoptosis in the cell lines by 2- to 5-fold relative to control (Fig. 2A). Equimolar concentration of ibuprofen did not appreciably induce apoptosis. Even at a concentration equal to 4 times that of PIA, ibuprofen only moderately induced apoptosis by <2-fold. PIA also inhibited cell cycle progression by arresting it at the G_1 phase (Fig. 2B). The G_1 phase cell population increased from 62.8% to 77.9% in A549 cells, 45.0–56.0% in H23 cells, and 51.0–62.1% in H358 cells after 24-h treatment with 0.75 × IC_{50} PIA. Ibuprofen, at 4 times the concentration of PIA, exhibited a comparable G_1 phase arresting effect in the H23 and H358 cell lines, but failed to do so in the A549 cells.

3.3. PIA inhibits the growth of lung cancer xenografts

To assess the *in vivo* efficacy of PIA against NSCLC, we treated athymic nude mice bearing orthotopic GFP-A549 xenografts ($n = 6$) with vehicle control or PIA administered i.p. Relative fluorescence intensity of GFP and lung weight were used to assess the antitumor efficacy of PIA (Fig. 3). The average tumor volume of the PIA-treated mice was 74% lower ($p < 0.001$) than that of the control group assessed by GFP luminosity at sacrifice. In addition, the average tumor weight of the PIA-treated group was 67% lower than that of the control. The average lung weight from another group of mice not implanted with cancer cells or subjected to vehicle or PIA treatment served as the normal control. Noticeably, the lung weight of the vehicle-treated group was 5.7-fold higher than that of normal mice. PIA i.p. treatment maintained lung weight of the mice near the normal levels. PIA also appeared to prevent health deterioration caused by the disease. By week 8, the average body weight of the PIA treatment group was essentially the same as that at baseline, whereas the vehicle control group had lost ∼30% of their body weights (Fig. 3B).

To test our hypothesis that PIA is metabolically stable *in vivo* and that intact PIA is the pharmacological active compound, we analyzed its pharmacokinetic profile in the plasma and its tissue distribution. In agreement with our expectations, intact PIA was the dominant compound detected in the blood and organs (Fig. 3C

A

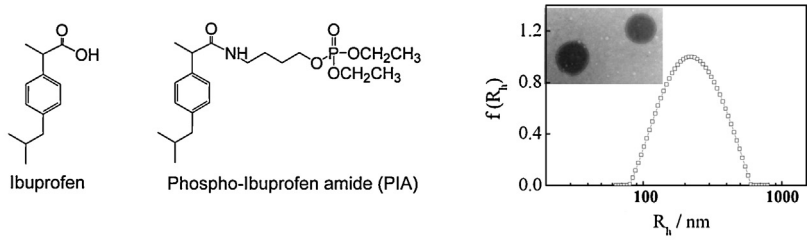

B

	Ibuprofen	PIA
Partition coefficient, log P	3.75	4.78
Cell uptake, nmol/mg protein	0.1±0.05	18±1.2
Liposomes		
Lipid/drug molar ratio	1.0/0	1.0/1.0
Cell uptake,nmol/mg protein	UD	82

UD: undetectable.

C

NSCLC cell line	24-h IC_{50}, μM		
	Ibuprofen	PIA	Fold enhancement
A549	2,500±280	202±57	10
H23	1543±206	172±31	9
H358	>6,000	401±42	>14

Fig. 1. Phospho-ibuprofen amide (PIA) is a more potent anticancer agent than ibuprofen *in vitro*. (A) PIA was formed by conjugation of ibuprofen to a diethyl phosphate group through an amide bond. *Left*: Ibuprofen and PIA. *Right*: Transmission electron microscopic image of liposomal PIA. (B) PIA is more hydrophobic than ibuprofen. A549 cells were treated with PIA or ibuprofen. Drug uptake was determined by HPLC and expressed as nmol/mg protein. PIA, but not ibuprofen, could be encapsulated in liposomes with a 1:1 lipid:drug ratio. (C) Cytotoxicity of ibuprofen and PIA in non-small-cell lung cancer cell lines. IC_{50} values were determined by the MTT assay and summarized in the table.

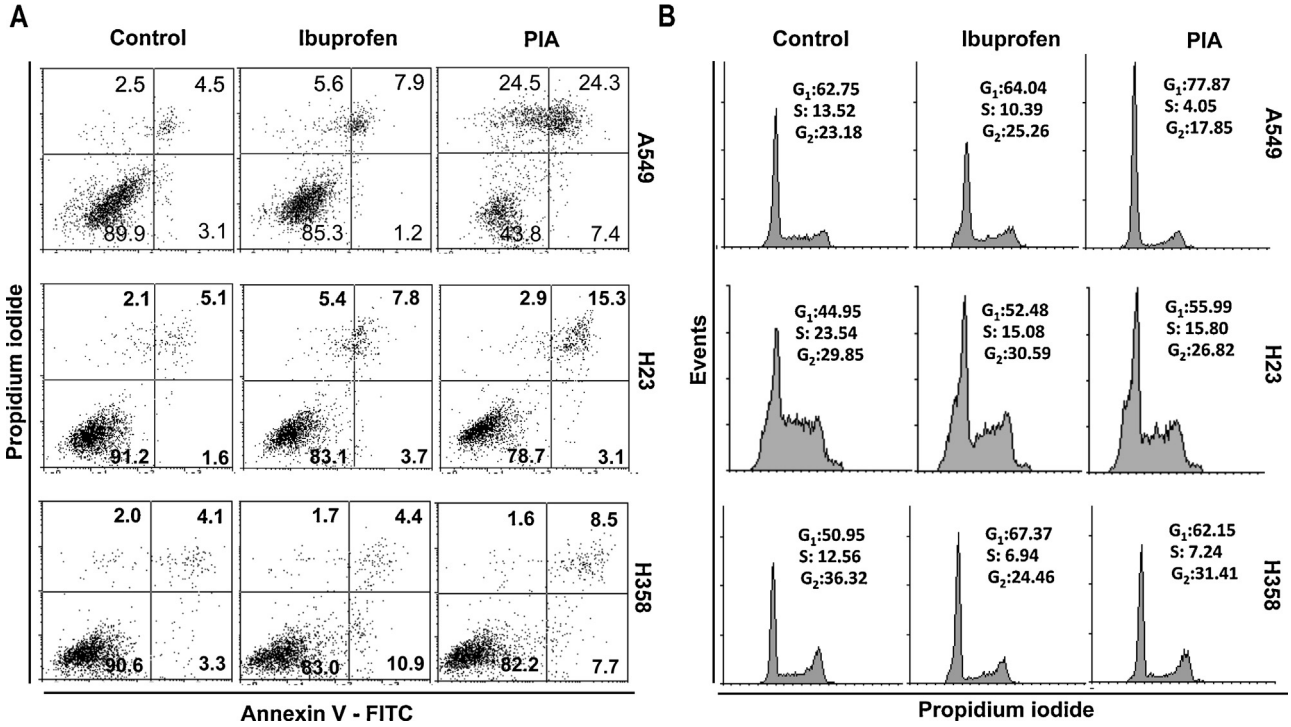

Fig. 2. The effect of PIA and ibuprofen on cytokinetics in NSCLC cell lines. Cells were treated with PIA or ibuprofen. (A) Apoptosis was determined by flow cytometry in cells stained with Annexin-V (abscissa) and PI (ordinate). PIA 1 × IC_{50} strongly induced apoptosis in A549 (*upper*), H23 (*middle*) and H358 (*bottom*) cells. Ibuprofen (4× the concentration of PIA) only moderately induced apoptosis. (B) Cell cycle analysis was performed on PI stained cells by flow cytometry. Percentages of cells in G1, S and G2 phases are shown in the histograms.

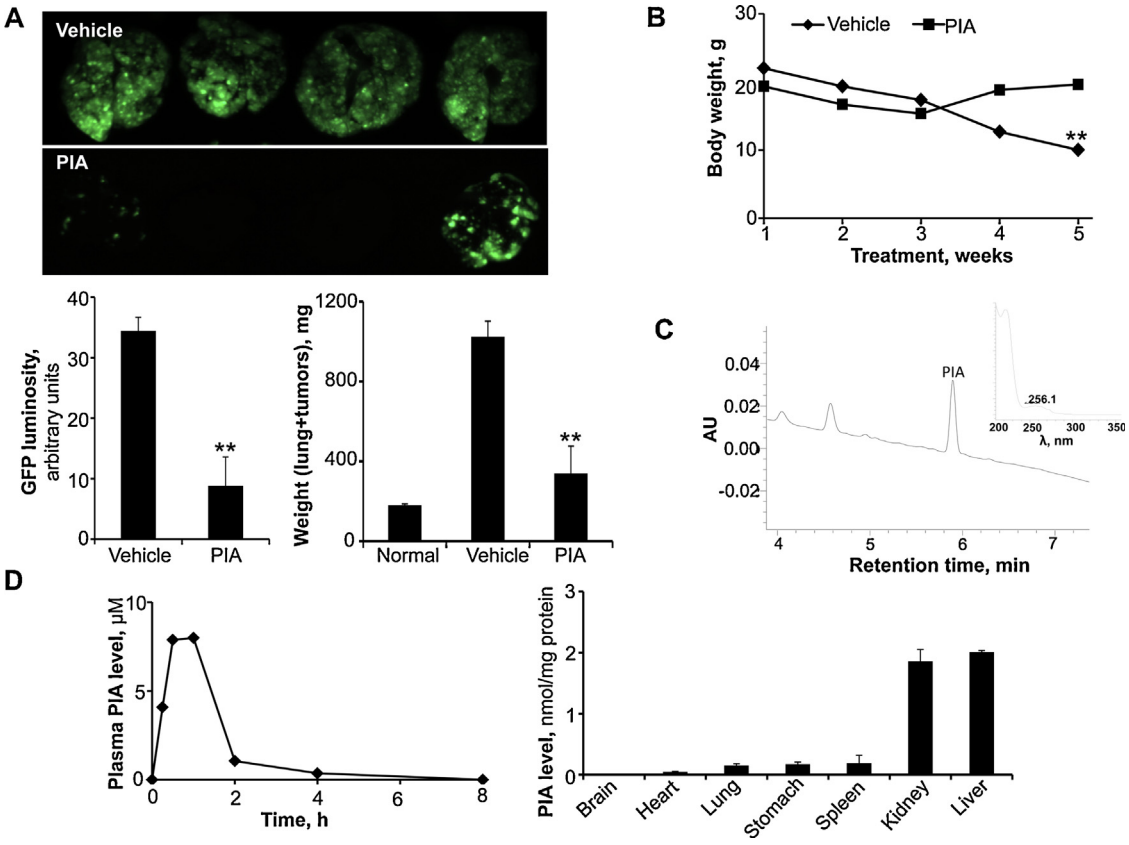

Fig. 3. Xenograft inhibitory effect and biodistribution of PIA in mice. GFP-transfected A549 cells (5×10^6) were injected into athymic nude mice through a tail vein. Treatment with vehicle or PIA (i.p. 200 mg/kg/day, 6 days/week) was started after two weeks when orthotopic tumors were established (monitored by *in vivo* imaging; Maestro, Wobum, MA). (A) PIA significantly (74%, $p < 0.001$) inhibited the growth of orthotopic lung cancer xenografts. *Upper*: Representative images of the lungs (cancerous and non-cancerous tissues) of mice from the vehicle and PIA-treated group at sacrifice, respectively. *Lower left*: GFP luminosity of the lungs of the vehicle vs. the PIA-treatment group. *Lower right*: Average lung weight of the vehicle and PIA-treatment group. (B) Change in body weights of the mice during the study period. (C) A representative HPLC chromatogram of a blood sample from a PIA-treated mouse and the UV-absorption spectrum of PIA. (D) Pharmacokinetic profiles of PIA in mice. Mice were treated with a single dose of PIA (i.p. 200 mg/kg) and euthanized at designated time points. Levels of PIA in the blood (*left*) and different organs (*right*) were determined by HPLC.

and D). The plasma level of PIA peaked 1 h post drug treatment, gradually decreased toward later time points and became undetectable after 4 h. These data suggest that the novel PIA is highly resistant to hydrolysis by carboxylesterases, in contrast to phospho-ibuprofen (Nie et al., 2012). It was also found that PIA administered by i.p. injection was predominantly subjected to liver/kidney metabolism/excretion, with only a small percentage (<5%) being delivered to the lungs.

3.4. Liposomal incorporation targets PIA to the lungs and enhances its anticancer activity

To explore the feasibility to selectively deliver PIA to the lungs by encapsulating it in liposomes, we evaluated the pharmacokinetics and tissue distribution of liposomal PIA in rats after a single i.v. administration of the drug (equivalent to 200 mg/kg PIA). In the plasma (Fig. 4A), intact PIA was the predominant form which peaked ($C_{max} = 5\ \mu M$) at 30 min, gradually decreased and was undetectable after 2.5 h. Tissue distribution analysis showed that liposomal PIA preferentially delivered PIA to the lungs, reaching 2.3 nmol/mg protein, which was significantly higher than the levels in other organs.

To assess whether the selective delivery of liposomal PIA to the lungs could be translated into enhanced anticancer activity, we tested the effect of i.v. liposomal PIA (200 mg/kg, once/week) on the growth of orthotopic A549 xenografts. We also compared its effect to that of ibuprofen. Remarkably, fluorescence imaging showed that liposomal PIA inhibited the growth of A549 xenografts by 95% ($p < 0.001$) relative to vehicle control (Fig. 4B). In addition, the average lung weight of the PIA-treated group was 80% lower than that of the control. At the equivalent dose, ibuprofen was much less effective, as indicated by only 55% reduction in GFP fluorescence and 20% reduction in lung weight compared to the control group. Of note, liposomal PIA was administered only once a week, which equated only one-sixth of the total drug dose of free PIA used in the other efficacy study. Thus, liposomal formulation proved to profoundly enhance the efficacy of PIA in inhibiting the growth of A549 lung cancer xenografts. IHC staining of paraffin-embedded lung cancer xenograft sections with PCNA showed that liposomal PIA significantly ($p < 0.05$) decreased the percentage of actively proliferating cells compared to controls (Fig. 4C).

3.5. PIA induces oxidative stress in vivo *and* in vitro

Our previous study (Sun et al., 2012) showed that phospho-ibuprofen induces oxidative stress in breast cancer cell lines by suppressing the thioredoxin (Trx) system, which plays an important role in mediating its anticancer activity. Hence, we analyzed the change of the status of oxidative stress in mice bearing A549 xenografts after treatment with PIA. The results showed that PIA given i.p. and liposomal PIA given i.v. both significantly ($p < 0.01$) induced oxidative stress *in vivo*, as reflected by the much higher levels of urinary 8-iso-$PGF_{2\alpha}$ in the PIA-treated group relative to control (Fig. 5A). Immunohistochemical staining of the orthotopic xenograft sections showed that PIA significantly

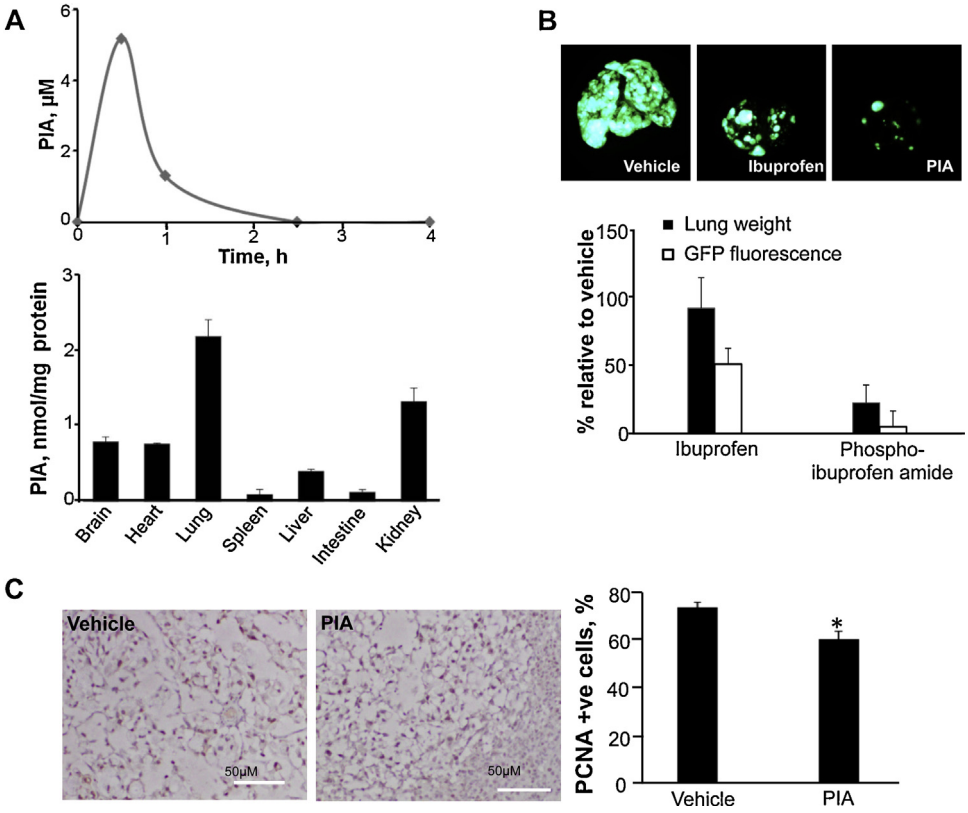

Fig. 4. Biodistribution of liposomal PIA and its xenograft inhibitory effect *in vivo*. (A) Pharmacokinetic profiles of liposomal PIA in rats. Rats were treated with a single dose of liposomal PIA (i.v. 200 mg/kg) and euthanized at designated time points. Levels of PIA in the blood (*upper*) and different organs (*lower*) were determined by HPLC. (B) GFP-transfected A549 cells (5×10^6) were injected into athymic nude mice through a tail vein. Treatment with vehicle, ibuprofen or PIA (i.v. 200 mg/kg/day, once/week) was started after two weeks when orthotopic tumors were established. *Upper*: Representative images of the lungs from the vehicle, ibuprofen, and liposomal PIA treatment group at sacrifice, respectively. *Lower*: Percent GFP luminosity and weight of the lungs (cancerous and non-cancerous tissues) from the ibuprofen and liposomal PIA treatment groups, relative to the vehicle control. (C) Immunostaining of paraffin-embedded tissue sections from the orthotopic A549 xenografts. Results are expressed as percentage positively stained cells. *Left*: Representative images of the PCNA-stained tissue sections from the vehicle and PIA-treated groups. . *Right*: Histogram showing percent PCNA-positive cells of the tissue sections from the vehicle and PIA treatment groups.

suppressed the expression of Trx-1 and Trx reductase (Fig. 5B), which likely contributed to the induction of oxidative stress *in vivo*.

In vitro, treatment of A549 cells with PIA at $1.5 \times IC_{50}$ for 1.5 h significantly induced the level of intracellular ROS by 4.9-fold (Fig. 5C). Further analysis revealed that PIA treatment also increased the levels of ROS in the H23 and H358 NSCLC cell lines by 17% and 65%, respectively. The equimolar doses of ibuprofen failed to induce ROS in these cell lines. Even at doses equal to 3–4 times those of PIA, ibuprofen was only able to induce ROS by 40%, 3%, and 8% in A549, H23 and H358 cells, respectively. These data suggest that the induction of oxidative stress may play an important role in mediating the activity of PIA against human NSCLC in pre-clinical models.

4. Discussion

The present study establishes that PIA is a novel agent with significantly improved anticancer activity over its parent NSAID, ibuprofen. The anticancer efficacy of PIA is mediated by (i) its potent cytokinetic effect on lung cancer cells; and (ii) its remarkable metabolic stability against esterase-mediated inactivation. Furthermore, incorporation of PIA into liposomes significantly enhanced its antitumor efficacy by improving its pharmacokinetics and targeting it to the lungs.

PIA is a potent inhibitor of lung cancer cell growth *in vitro* (~10-fold more potent than ibuprofen). PIA exerts a potent cytokinetic effect, which is a result of induction of apoptosis, inhibition of cell proliferation and of cell cycle progression (G_0/G_1). *In vivo*, PIA suppressed the growth of orthotopic A549 lung tumors (75% inhibition) in immunodeficient mice, and this effect was further enhanced (95% inhibition) by its formulation in liposomes. The parent NSAID ibuprofen was much less efficacious, inhibiting tumor growth by about half (55%). These results indicate that, PIA, especially liposome-incorporated PIA, is a potent inhibitor of lung cancer.

Our data suggest the induction of oxidative stress as an important mechanism of cell death caused by PIA. This effect was noted both in cultured cells, by using the ROS probe DCF-DA, and in animals, by assaying urinary levels of 8-iso-$PGF_{2\alpha}$, a widely used marker of oxidative stress *in vivo* (Milne et al., 2005). This finding is in agreement with previous studies (Huang et al., 2010; Mackenzie et al., 2010, 2011), which showed that ROS induction is a pivotal event in the anticancer effect of phospho-NSAIDs. Cancer cells are often in a heightened state of oxidative stress (Diehn et al., 2009). Hence, they are vulnerable to excess ROS (Fruehauf and Meyskens, 2007), and the induction of ROS may underlie the potent effect of PIA in suppressing tumor growth.

A critical contributing factor to the potent anticancer activity of PIA is its metabolic stability. PIA is an amide derivative of phospho-ibuprofen. Phospho-ibuprofen, whilst being considerably more cytotoxic toward cancer cells than ibuprofen, displayed only moderately improved efficacy *in vivo*. *In vivo,* phospho-NSAIDs are susceptible to hydrolysis at their carboxylic ester bond by carboxylesterases in the liver, intestine or plasma (Nie et al., 2012). Phospho-ibuprofen, for example, is rapidly hydrolyzed by carboxylesterase 1 to give the considerably less active ibuprofen

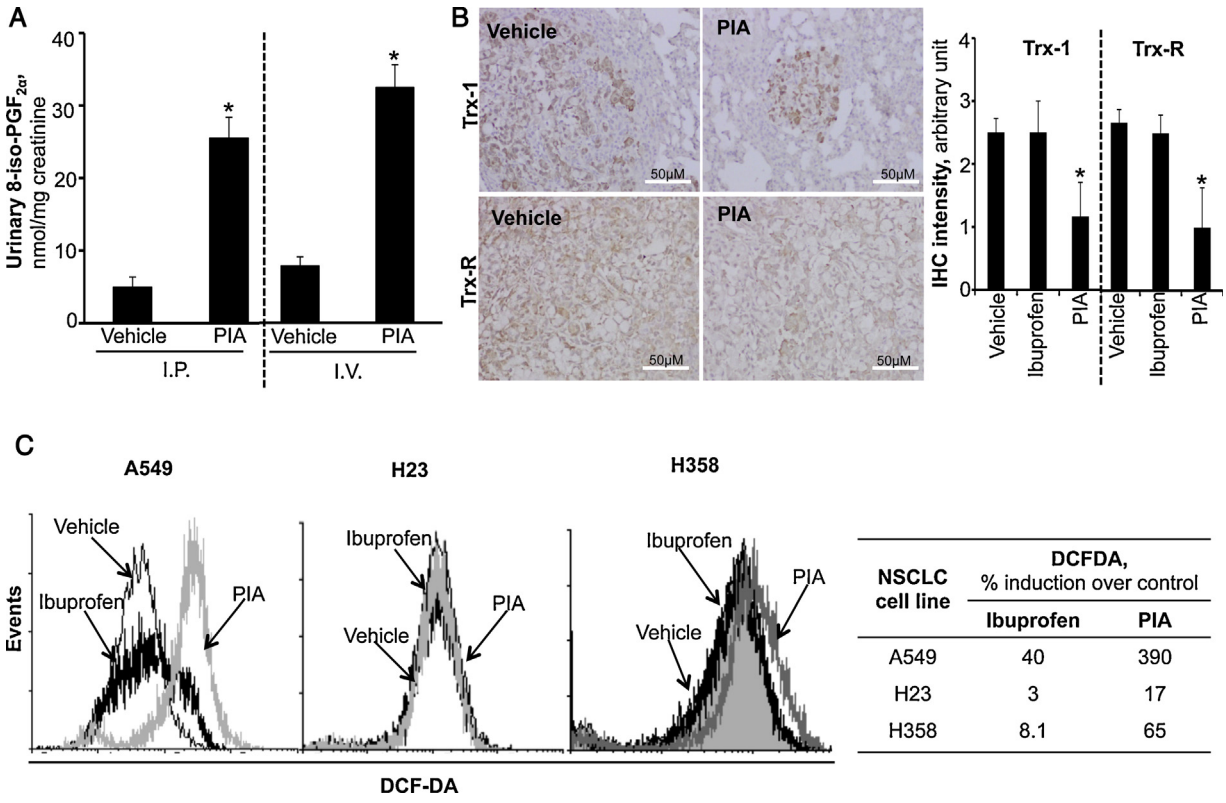

NSCLC cell line	DCFDA, % induction over control	
	Ibuprofen	PIA
A549	40	390
H23	3	17
H358	8.1	65

Fig. 5. PIA induces oxidative stress *in vivo and in vitro*. (A) Urinary 8-iso-prostaglandin $F_{2\alpha}$ (8-iso-$PGF_{2\alpha}$) levels of athymic nude mice bearing A549 xenografts treated with vehicle or PIA. *Left*: PIA, i.p. 200 mg/kg/day, 6 days/week for 6 weeks. *Right*: i.v. 200 mg/kg/day, once/week for 6 weeks. (B) Immunostaining of paraffin-embedded tissue sections from the orthotopic A549 xenografts. *Upper left*: Representative images of Trx-1 stained tissue sections. *Lower left*: Representative images of Trx-R stained tissue sections. *Right*: Histograms showing IHC scores of the tissue sections from the different treatment groups. (C) PIA induced ROS in A549, H23 and H358 cells more potently than ibuprofen. Cells were treated with PIA 1.5 × IC_{50} or ibuprofen (4× the concentration of PIA) for 1.5 h, stained with DCF-DA and analyzed by flow cytometry. *Left*: Histograms showing the induction of ROS by PIA vs. ibuprofen in different NSCLC cell lines. Percentages of ROS induction by PIA and by ibuprofen are summarized in the table.

(Wong et al., 2012). PIA, on the other hand, exhibits remarkable metabolic stability, as manifested in its resistance to hydrolysis by carboxylesterases. As a consequence, PIA evades carboxylesterase-mediated inactivation and remains predominantly intact in the circulation of mice, thereby improving the delivery of the potent, intact drug to lung tumors.

The phospho-modification has an important impact on the physicochemical properties of NSAIDs. PIA is significantly more hydrophobic than ibuprofen and is only sparsely soluble in water. This property allows PIA to permeate cell membranes readily (confirmed by the 180-fold enhanced cellular uptake), but it limits bioavailability and prevents the use of i.v. administration due to the high risk of drug aggregation in the circulation. Although i.p. administration of PIA demonstrated much better bioavailability than the oral route (data not shown), it did not result in preferential drug delivery to the lungs. Therefore, the therapeutic efficacy achieved with i.p. delivery was sub-optimal.

The anticancer efficacy of PIA can be augmented through incorporation into liposomes. Nanocarriers, such as liposomes, are well-established vehicles for the solubilization of hydrophobic drugs and for improving pharmacokinetic properties. We have demonstrated highly efficient loading of PIA in liposomes, with a drug:lipid ratio of 1:1. The incorporation of PIA into liposomes increased its already superior ability to penetrate cells compared to ibuprofen *in vitro*. *In vivo* biodistribution studies indicate that liposomal PIA was preferentially delivered to the lungs, resulting in higher levels than those in other organs. A recent study (Wei et al., 2014) reported the capability of liposomes to alter the biodistribution of paclitaxel, manifested in the significantly enhanced delivery of the drug to the lungs by a factor of 14–20 compared to other organs. The authors thus proposed liposome to be a promising carrier to target the anticancer drug to the lungs for lung cancer treatment. Because of the targeted delivery, i.v. administration of liposomal PIA only required one-sixth of the dosage of free PIA given by i.p. over the study period to achieve the nearly complete tumor elimination. In addition, liposomes facilitate tumor targeting via the enhanced permeability and retention (EPR) effect whereby they extravasate through the "leaky" vasculature of tumors (Maeda et al., 2000). All these factors may contribute to the potent efficacy and enhanced therapeutic index of liposomal PIA in the inhibition of lung tumor growth.

In conclusion, our findings suggest that PIA is a promising agent against human NSCLC and that liposomes enhance its intrinsic anticancer effect, greatly improving its therapeutic index.

References

Alexis, F., Pridgen, E.M., Langer, R., Farokhzad, O.C., 2010. Nanoparticle technologies for cancer therapy. Handb. Exp. Pharmacol. 55–86.
Blanco, E., Kessinger, C.W., Sumer, B.D., Gao, J., 2009. Multifunctional micellar nanomedicine for cancer therapy. Exp. Biol. Med. (Maywood) 234, 123–131.
Blanco, E., Bey, E.A., Khemtong, C., Yang, S.G., Setti-Guthi, J., Chen, H., Kessinger, C.W., Carnevale, K.A., Bornmann, W.G., Boothman, D.A., Gao, J., 2010. Beta-lapachone micellar nanotherapeutics for non-small cell lung cancer therapy. Cancer Res. 70, 3896–3904.
Diehn, M., Cho, R.W., Lobo, N.A., Kalisky, T., Dorie, M.J., Kulp, A.N., Qian, D., Lam, J.S., Ailles, L.E., Wong, M., Joshua, B., Kaplan, M.J., Wapnir, I., Dirbas, F.M., Somlo, G., Garberoglio, C., Paz, B., Shen, J., Lau, S.K., Quake, S.R., Brown, J.M., Weissman, I.L., Clarke, M.F., 2009. Association of reactive oxygen species levels and radioresistance in cancer stem cells. Nature 458, 780–783.
Flenniken, M.L., Willits, D.A., Harmsen, A.L., Liepold, L.O., Harmsen, A.G., Young, M.J., Douglas, T., 2006. Melanoma and lymphocyte cell-specific targeting incorporated into a heat shock protein cage architecture. Chem. Biol. 13, 161–170.

Fruehauf, J.P., Meyskens Jr., F.L., 2007. Reactive oxygen species: a breath of life or death? Clin. Cancer Res. 13, 789–794.
Gabizon, A.A., 2001. Pegylated liposomal doxorubicin: metamorphosis of an old drug into a new form of chemotherapy. Cancer Invest. 19, 424–436.
Harris, R.E., Beebe-Donk, J., Alshafie, G.A., 2007. Reduced risk of human lung cancer by selective cyclooxygenase 2 (COX-2) blockade: results of a case control study. Int. J. Biol. Sci. 3, 328–334.
Henry, D., McGettigan, P., 2003. Epidemiology overview of gastrointestinal and renal toxicity of NSAIDs. Int. J. Clin. Pract. Suppl. 43–49.
Huang, L., Zhu, C., Sun, Y., Xie, G., Mackenzie, G.G., Qiao, G., Komninou, D., Rigas, B., 2010. Phospho-sulindac (OXT-922) inhibits the growth of human colon cancer cell lines: a redox/polyamine-dependent effect. Carcinogenesis 31, 1982–1990.
Huang, L., Mackenzie, G.G., Sun, Y., Ouyang, N., Xie, G., Vrankova, K., Komninou, D., Rigas, B., 2011. Chemotherapeutic properties of phospho-nonsteroidal anti-inflammatory drugs, a new class of anticancer compounds. Cancer Res. 71, 7617–7627.
Jemal, A., Siegel, R., Xu, J., Ward, E., 2010. Cancer statistics: 2010. CA Cancer J. Clin. 60, 277–300.
Kozoni, V., Tsioulias, G., Shiff, S., Rigas, B., 2000. The effect of lithocholic acid on proliferation and apoptosis during the early stages of colon carcinogenesis: differential effect on apoptosis in the presence of a colon carcinogen. Carcinogenesis 21, 999–1005.
Lee, C.C., MacKay, J.A., Frechet, J.M., Szoka, F.C., 2005. Designing dendrimers for biological applications. Nat. Biotechnol. 23, 1517–1526.
Mackenzie, G.G., Sun, Y., Huang, L., Xie, G., Ouyang, N., Gupta, R.C., Johnson, F., Komninou, D., Kopelovich, L., Rigas, B., 2010. Phospho-sulindac (OXT-328), a novel sulindac derivative, is safe and effective in colon cancer prevention in mice. Gastroenterology 139, 1320–1332.
Mackenzie, G.G., Ouyang, N., Xie, G., Vrankova, K., Huang, L., Sun, Y., Komninou, D., Kopelovich, L., Rigas, B., 2011. Phospho-sulindac (OXT-328) combined with difluoromethylornithine prevents colon cancer in mice. Cancer Prevent. Res. 4, 1052–1060.
Maeda, H., Wu, J., Sawa, T., Matsumura, Y., Hori, K., 2000. Tumor vascular permeability and the EPR effect in macromolecular therapeutics: a review. J. Control Release 65, 271–284.
Mattheolabakis, G., Nie, T., Constantinides, P.P., Rigas, B., 2012. Sterically stabilized liposomes incorporating the novel anticancer agent phospho-ibuprofen (MDC-917): preparation, characterization, and in vitro/in vivo evaluation. Pharm. Res. 29, 1435–1443.
Milne, G.L., Musiek, E.S., Morrow, J.D., 2005. F2-isoprostanes as markers of oxidative stress in vivo: an overview. Biomarkers 10, S10–S23.
Nie, T., Wong, C.C., Alston, N., Aro, P., Constantinides, P.P., Rigas, B., 2012. Phospho-ibuprofen (MDC-917) incorporated in nanocarriers: anti-cancer activity in vitro and in vivo. Br. J. Pharmacol. 166, 991–1001.
Peer, D., Karp, J.M., Hong, S., Farokhzad, O.C., Margalit, R., Langer, R., 2007. Nanocarriers as an emerging platform for cancer therapy. Nat. Nanotechnol. 2, 751–760.
Sun, Y., Rowehl, L.M., Huang, L., Mackenzie, G.G., Vrankova, K., Komninou, D., Rigas, B., 2012. Phospho-ibuprofen (MDC-917) suppresses breast cancer growth: an effect controlled by the thioredoxin system. Breast Cancer Res. 14, R20.
Sutton, D., Nasongkla, N., Blanco, E., Gao, J., 2007. Functionalized micellar systems for cancer targeted drug delivery. Pharm. Res. 24, 1029–1046.
Wei, Y., Xue, Z., Ye, Y., Huang, Y., Zhao, L., 2014. Paclitaxel targeting to lungs by way of liposomes prepared by the effervescent dispersion technique. Arch. Pharm. Res. 37, 728–737.
Wolfe, M.M., Lichtenstein, D.R., Singh, G., 1999. Gastrointestinal toxicity of nonsteroidal antiinflammatory drugs. N. Engl. J. Med. 340, 1888–1899.
Wong, C.C., Cheng, K.W., Xie, G., Zhou, D., Zhu, C.H., Constantinides, P.P., Rigas, B., 2012. Carboxylesterases 1 and 2 hydrolyze phospho-nonsteroidal anti-inflammatory drugs: relevance to their pharmacological activity. J. Pharmacol. Exp. Ther. 340, 422–432.
Xie, G., Sun, Y., Nie, T., Mackenzie, G.G., Huang, L., Kopelovich, L., Komninou, D., Rigas, B., 2011. Phospho-ibuprofen (MDC-917) is a novel agent against colon cancer: efficacy, metabolism, and pharmacokinetics in mouse models. J. Pharmacol. Exp. Ther. 337, 876–886.
Yoshikawa, T., Naito, Y., 2011. Pathogenesis of NSAIDs-induced gastrointestinal ulcers. Nihon rinsho 69, 995–1002.